

Corrected: Publisher Correction

OPEN

DATA DESCRIPTOR

Gaze, visual, myoelectric, and inertial data of grasps for intelligent prosthetics

Matteo Cognolato ^{1,2*}, Arjan Gijsberts³, Valentina Gregori^{3,4}, Gianluca Saetta ⁵, Katia Giacomino⁶, Anne-Gabrielle Mittaz Hager⁶, Andrea Gigli³, Diego Faccio⁷, Cesare Tiengo⁷, Franco Bassetto⁷, Barbara Caputo^{3,8}, Peter Brugger^{5,9}, Manfredo Atzori^{1*} & Henning Müller ^{1,10*}

A hand amputation is a highly disabling event, having severe physical and psychological repercussions on a person's life. Despite extensive efforts devoted to restoring the missing functionality via dexterous myoelectric hand prostheses, natural and robust control usable in everyday life is still challenging. Novel techniques have been proposed to overcome the current limitations, among them the fusion of surface electromyography with other sources of contextual information. We present a dataset to investigate the inclusion of eye tracking and first person video to provide more stable intent recognition for prosthetic control. This multimodal dataset contains surface electromyography and accelerometry of the forearm, and gaze, first person video, and inertial measurements of the head recorded from 15 transradial amputees and 30 able-bodied subjects performing grasping tasks. Besides the intended application for upper-limb prosthetics, we also foresee uses for this dataset to study eye-hand coordination in the context of psychophysics, neuroscience, and assistive robotics.

Background & Summary

The human hand has a fundamental role in many aspects of everyday life. Its morphological structure not only makes it one of the distinctive characteristics of the human species, but it also provides us with unique manipulative abilities^{1,2}. We use it to sense and interact with the environment and it has an essential role in social interactions and communication. Losing a hand therefore has severe physical and psychological consequences on a person's life. Myoelectric hand prostheses have enabled amputees to restore some of the missing functionality. In their conventional form, prostheses use surface electromyography (sEMG) from an antagonist pair of muscles to open and close a simple gripper. A large number of pattern recognition (PR) approaches have been developed over the years aiming to increase the functionality and control of more dexterous prostheses³⁻⁵. Despite these efforts, PR-based prostheses have not managed to deliver their full potential in practical clinical applications^{6,7}. One of the primary causes is that they are sensitive to the variability of sEMG, limiting the robustness and reliability in long-term practical applications^{4,8-14}. This limitation is inherent in the use of sEMG as a control modality, since myoelectric signals are known to depend on factors such as electrode displacement, inconsistency of the skin-electrode interface, changes in arm position, and characteristics of the amputation.

Several techniques have been proposed to address this variability and thus improve the stability of the prosthetic control^{4,11,15,16}. One approach relies on fusing sEMG with complementary sources of information, such as gaze and computer vision¹⁷⁻²⁰. Studies on eye-hand coordination have in fact shown that gaze typically anticipates and guides grasping and manipulation²¹⁻²³. In other words, humans will look at an object they intend to grasp before executing the movement itself. Gaze behavior therefore holds valuable information for recognizing not

¹Information Systems Institute, University of Applied Sciences Western Switzerland (HES-SO Valais), Sierre, Switzerland. ²Rehabilitation Engineering Laboratory, Department of Health Sciences and Technology, ETH Zurich, Zurich, Switzerland. ³Istituto Italiano di Tecnologia, Genoa, Italy. ⁴Department of Computer, Control, and Management Engineering, University of Rome La Sapienza, Rome, Italy. ⁵Department of Neurology, University Hospital of Zurich, Zurich, Switzerland. ⁶Department of Physical Therapy, University of Applied Sciences Western Switzerland (HES-SO Valais), Leukerbad, Switzerland. ⁷Clinic of Plastic Surgery, Padova University Hospital, Padova, Italy. ⁸Politecnico di Torino, Turin, Italy. ⁹Rehabilitation Center Valens, Valens, Switzerland. ¹⁰University of Geneva, Geneva, Switzerland. *email: matteo.cognolato@hevs.ch; manfredo.atzori@hevs.ch; henning.mueller@hevs.ch

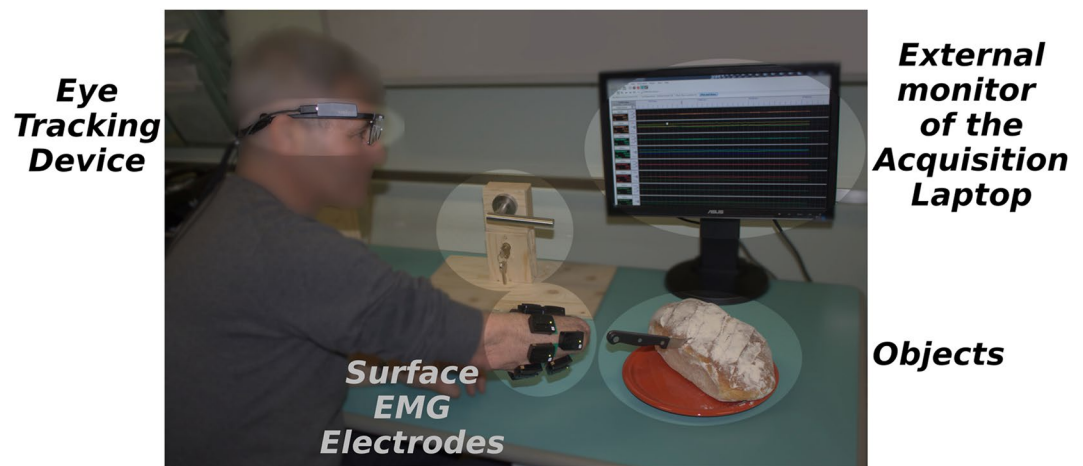


Fig. 1 Overall view of the acquisition setup.

only the intention to grasp an object, but also to identify *which* object the person intends to grasp. The set of likely grasps can then be estimated based on the size, shape, and affordances of this object. For large objects, this may be further refined by considering the exact part or side of the object on which the person fixates.

There are two compelling motivations for using gaze behavior in the context of upper limb prosthetics. The first is that gaze behavior is not necessarily affected by the amputation. Any information on muscular activation recorded from the residual limb, such as sEMG, is inherently degraded due to muscular reorganization after the amputation and subsequent atrophy due to reduced use. The second advantage is that integrating some level of autonomy in a prosthesis can lower the physical and psychological burden placed on its user. Fatigue is one of the causes of variability in sEMG data^{24–26}, so reducing it can help to stabilize control.

This paper presents the MeganePro dataset 1 (MDS1) acquired during the MeganePro project, which was designed based on the experience gained during the NinaPro project²⁷. The goals of the MeganePro project were to investigate the use of gaze and computer vision to improve the control of myoelectric hand prostheses for transradial amputees, and to better understand the neurocognitive effects of amputation. This dataset was acquired to explore the first goal: it contains multimodal data from 15 transradial amputees and 30 able-bodied subjects while involved in grasping and manipulating objects using 10 common grasps. Throughout the exercise, we acquired sEMG and accelerometry using twelve electrodes on the forearm. Gaze, first person video, and inertial measurements of the head were recorded using eye tracking glasses.

In the following sections, we describe the experimental protocol, the processing procedures, and the resulting data records. Although prosthetic control was our motivation for acquiring this dataset, it is our belief that the data will find broader applications. For instance, scientists working in neuroscience, psychophysics, or rehabilitation robotics may use it to study gaze and manipulation independently as well as via their coordination. In particular, the data allow direct comparison of able-bodied subjects and transradial amputees in an identical experimental setting. As such, it may contribute not only to develop better prostheses but also a better understanding of human behavior and the implications of amputation.

Methods

The acquisition of the dataset consisted of defining an experimental protocol and determining the requirements in terms of devices and software. A general overview of the setup and protocol is shown in Fig. 1. Once the ethical approval was obtained, we proceeded with subject recruitment. In the following, all these phases are described in detail.

Ethical Requirements. The experiment was designed and conducted in accordance with the principles expressed in the Declaration of Helsinki. Ethical approval for our study was requested to and approved by the Ethics Commission of the canton of Valais in Switzerland (CCVEM 010/11) and by the Ethics Commission of the Province of Padova in Italy (NRC AOP1010, CESC 4078/AO/17). Prior to the experiment, each subject was given a detailed written and oral explanation of the experimental setup and protocol. They were then required to give informed consent to participate in the research study.

Subject Recruitment. A total of 15 transradial amputees and 30 able-bodied subjects were recruited for this study. The former group consists of 13 male and 2 female (13.3%) participants with an average age of (47.13 ± 14.16) years. As seen in Table 1, among them are diverse causes for amputation and different preferences with respect to prosthetic use. To remove possible confounding variables, we recruited a control group of able-bodied participants that matched the former group as much as possible in terms of age and gender. This group is composed of 27 male and 3 female (10.0%) subjects, with an average age of (46.63 ± 15.11) years.

Acquisition Setup. We designed an acquisition setup that allowed us to perform eye tracking and to acquire sEMG from the forearm, while leaving the subjects as free as possible in their movements. Custom developed

	ID	Age	Gender	Handedness	Language	Amputation Side	Amputation Cause	Years since Amputation	Prosthesis	Residual Limb Length [%]
Transradial Amputees	101	52	M	right	IT	right	electrocution	2	cosmetic	60–80
	102	39	M	right	IT	right	electrocution	4	cosmetic	60–80
	103	63	M	ambidextrous	IT	right	trauma	3	myoelectric	60–80
	104	49	M	right	IT	right	trauma	18	myoelectric	80–100
	105	73	M	right	IT	right	trauma	6	body-powered	40–60
	106	70	M	left	IT	left	trauma	5	body-powered	80–100
	107	36	M	right	IT	left	trauma	7	body-powered	20–40
	108	35	M	right	IT	right	trauma	9	myoelectric	0–20
	109	65	M	right	IT	left	trauma	1	cosmetic	80–100
	110	38	M	right	IT	left	trauma	14	myoelectric	20–40
	111	38	M	right	IT	right	trauma	10	myoelectric	40–60
	112	33	F	right	IT	left	oncological	13	cosmetic	60–80
	113	28	M	right	IT	left	trauma	7	myoelectric	40–60
	114	52	M	right	IT	bilateral	trauma	35	myoelectric	n/a
	115	36	F	right	IT	left	burn	8	cosmetic	n/a
Able-bodied Subjects	10	27	M	right	EN					
	11	63	M	right	FR					
	12	49	M	right	FR					
	13	32	M	left	FR					
	14	67	M	right	DE					
	15	68	M	right	DE					
	16	38	M	right	FR					
	17	63	M	ambidextrous	FR					
	18	55	M	right	FR					
	19	29	M	right	FR					
	20	48	M	left	FR					
	21	62	M	left	FR					
	22	39	M	right	FR					
	23	53	M	right	FR					
	24	29	M	right	FR					
	26	45	M	right	FR					
	27	68	M	right	FR					
	28	62	M	right	FR					
	29	58	M	right	FR					
	30	66	M	right	FR					
31	39	M	right	FR						
32	34	M	right	EN						
33	69	M	right	FR						
34	57	M	right	DE						
35	29	F	ambidextrous	EN						
36	28	M	right	IT						
37	31	M	right	EN						
38	29	F	right	EN						
39	33	F	ambidextrous	EN						
40	29	M	right	FR						

Table 1. Participant characteristics. The table reports the ID of the subjects in the dataset, their age, gender, and handedness. Clinical parameters about the amputation(s) are also reported for the transradial amputees. The rightmost column indicates the relative length of the residual limb with respect to the contralateral limb. IT stands for Italian, EN for English, FR for French, DE for German, and n/a for “not applicable”.

software interfaced with the acquisition devices and provided stimuli instructing the subjects when to grasp which object.

Sensors. The electrical activity of the forearm muscles was recorded with a Delsys Trigno Wireless sEMG System (Delsys Inc., USA, <http://www.delsys.com/>). This system consists of sEMG electrodes with an inter-sensor latency lower than 500 μ s and a signal baseline noise lower than 750 nV Root Mean Square (RMS). In addition,

a three-axial accelerometer is embedded in each electrode. Up to 16 electrodes communicate wirelessly with the base station, which is connected through a USB 2.0 cable to the acquisition laptop. The sEMG data are sampled at 1926 Hz and the accelerometer at 148 Hz. The accelerometer range was set at ± 1.5 g, for which the device documentation reports a noise of 0.007 g RMS. The corresponding offset error is ± 0.201 g for the X and Y axes and (0.201 to -0.343) g for the Z axis²⁸.

The gaze behavior and first person video were recorded with the Tobii Pro Glasses 2 (Tobii AB, Sweden, <http://www.tobii.com/>). The head unit of this device is similar to regular eyeglasses and equipped with four eye cameras recording the eye movement, a camera capturing the scene in front of the subject, an Inertial Measurement Unit (IMU), and a microphone. It weighs only 45 g and corrective lenses can be applied for subjects with visual deficit. The eyes are tracked using corneal reflection and dark pupil methods with automatic parallax and slippage compensation. These eye tracking data are sampled at 100 Hz with a theoretical accuracy and precision of 0.5° and 0.3° RMS²⁹. Video with Full HD resolution (1920 px \times 1080 px) is recorded at 25 fps by the scene camera with a horizontal and vertical field of view of approximately 82° and 52°. The head unit is connected via a cable to a portable recording unit that is responsible for transmitting the data wirelessly and storing them on a memory card. A rechargeable and replaceable battery powers both head and recording units and provides a maximum recording time of approximately 120 min. The system can quickly and easily be calibrated with a single point calibration procedure.

Acquisition Software. The role of the acquisition software is to simultaneously acquire and store the data from all sensor devices, and to guide the subject through the exercises. To ensure high performance and low latency, the application was developed in C++ and based on the multithreaded producer-consumer pattern, as implemented in CEINMS³⁰. More specifically, for each data source there is a dedicated producer thread responsible for acquiring its data, assigning a high-resolution timestamp, and then storing these in a queue. Per queue there is at least one consumer thread that stores available data to a file. The advantage of this architecture is that it uncouples the data acquisition from I/O latency when saving the data to a persistent storage.

A Graphical User Interface (GUI) developed in Qt5 (<https://www.qt.io/>) was added to the application to demonstrate using videos and images how to perform the exercises. In previous studies, such as NinaPro²⁷, the subjects had to mimic a grasp movement that was shown in a video. This approach is not compatible with the present study, since it influences the subject's gaze behavior. We therefore opted to avoid the need for visual attention and to instruct the subjects via vocal instructions during the real exercise. These instructions were automatically synthesized by a text-to-speech engine, which allowed us to prepare instructions in English, Italian, French, and German. At the start of the exercise subjects could choose the language they were most comfortable with.

Grasp Types and Objects. A total of ten grasp types were selected for our exercise from well-known hand taxonomies^{31–34} based on their relevance for Activities of Daily Living (ADLs)³⁵. These grasp types were then matched with three household objects each that would regularly be manipulated using a given grasp. An overview of the ten grasp types and eighteen objects is given in Table 2. When possible, these pairings were chosen to obtain a many-to-many relationship between objects and grasp types; that is, a grasp could be used with multiple objects and vice versa. This requirement helped to limit the possibility that the mere presence of an object would be sufficient to unequivocally determine the grasp type.

In the case that an object is not usually found on a table (e.g., a door handle or a door lock), a custom made support was created. To avoid complications during the exercise, the key, bulb, lid of the jar, and the screw used with the screwdriver were modified such that they could not be completely removed from the support. Furthermore, the pull tab of the can was bent to facilitate the execution of the grasp.

During the exercise, at least five objects were simultaneously placed in the scene with a predefined position. The presence of multiple objects in front of the subjects helped to simulate a real environment, while a standardized object arrangement minimized the possibility of an error during the placement of the objects. In addition, these objects were spread throughout the subject's reachable workspace so that grasps had to be performed while reaching in various directions.

Acquisition Protocol. After the ethical requirements were fulfilled, the subject's data, such as age, gender, height, weight, and handedness were collected. The amputees were asked additional information regarding the amputation, such as cause, type, years since amputation, and prosthesis use. A summary of this information is reported in Table 1.

The subjects were asked to sit with the forearm comfortably leaning on a desk and, for amputees, to remove the prosthesis. The skin was cleaned with isopropyl alcohol and twelve sEMG electrodes were placed in two arrays around the right forearm or residual limb. An array of eight electrodes was placed equidistantly around the forearm, starting at the radio-humeral joint and moving in the direction of pronation. A second array was located approximately 45 mm more distally and aligned with the gaps between electrodes one and two, three and four, and so on (see Fig. 1). In addition to the Trigno-specific adhesive strips, a latex-free elastic band was wrapped around the electrodes to assure a good and reliable interface with the skin. As widely done in the field of PR myoelectric control, the sEMG electrodes were placed around the proximal part of the forearm, where most of the extrinsic muscles of the hand lie, following an *untargeted approach*⁵. This approach consists of several equidistantly placed electrodes, recording the forearm (intact or residual) musculature's electrical activity from multiple sEMG sites, without targeting any specific muscles or muscle parts³⁶.

The subject was then asked to wear the Tobii Pro glasses, where we made sure to choose the nose pad that aligned the eye tracking cameras' appropriately. Once the subject felt ready, the Tobii Pro glasses were calibrated using the built-in one point target calibration procedure and, in case of success, the subject was asked to perform a calibration assessment. This assessment consisted in asking the subject to fixate a black cross against a green

Grasp		Object		Object Part		Vocal Instruction	
1	medium wrap	1	bottle	1	bottle	take the bottle	
		2	can	2	can		can
		3	door handle	3	door handle		door handle
2	lateral	4	mug	23	handle		mug
		5	key	5	key		key
		24	pencil case	6	zip		zip
3	parallel extension	7	plate	7	plate		plate
		8	book	8	book		book
		9	drawer	9	drawer		drawer
4	tripod grasp	1	bottle	10	cap		cap of the bottle
		4	mug	4	mug		mug
		9	drawer	11	knob		knob of the drawer
5	power sphere	12	ball	12	ball		ball
		13	bulb	13	bulb		light bulb
		5	key	5	key		keys
6	precision disk	15	jar	26	lid		jar
		13	bulb	13	bulb		light bulb
		12	ball	12	ball		ball
7	prismatic pinch	16	clothespin	16	clothespin		clothespin
		5	key	27	keyring		keys
		2	can	25	pull tab		can
8	index finger extension	21	remote	17	button	point at a button of the remote	
		18	knife	18	knife	take the knife	
		19	fork	19	fork		fork
9	adducted thumb	20	screwdriver	20	screwdriver		screwdriver
		21	remote	21	remote		remote
		22	wrench	22	wrench		wrench
10	prismatic four finger	18	knife	18	knife		knife
		19	fork	19	fork		fork
		22	wrench	22	wrench		wrench

Table 2. Overview of the grasp types and objects for the *static* condition of the exercise. The columns indicate the ID and name of the grasp as commonly reported literature^{31,34}, the ID and name of the object, and in some cases a further refinement indicating the ID and name of the part of the object that was involved in the grasping. The fourth column reports the vocal command given to the subject.

background that was displayed on a monitor at a distance of about 1.3 m. This cross remained fixed for 3 s in the same location before alternating to another one out of five positions in total.

The actual exercise consisted of repeatedly executing the grasps on the set of corresponding objects, as described in Table 2. In the first part, which we refer to as *static*, subjects were requested to grasp the objects without actually moving or lifting them. Prior to executing a grasp, videos in first and third person perspectives demonstrated the grasp and the three corresponding objects. The subjects were however instructed to execute the movements spontaneously, rather than trying to mimic the exact kinematics of the demonstration videos. Amputees were asked to attempt executing the movements as naturally as possible, as they would intuitively *perform the grasp with the missing hand*. During these videos, the subject was free to decide whether to perform or not the grasps to get confident about the exercise. Once the grasp and objects had been shown, the subject had to repeat each combination four times while seated and then another four times while standing. This change in position was intended to include variability in the limb position in the data. The duration of the movement and rest periods depends on the selected language for the vocal instructions. A grasp interval lasted approximately 5.2 s, 5.7 s, 5.9 s, and 6.0 s for English, Italian, French, and German. A rest period followed for about 4.1 s, 4.7 s, 4.7 s, and 4.7 s for English, Italian, French, and German. The exact order of the objects within each repetition was randomized to avoid learning and habituation effects. A vocal command guided the subject through the exercise, indicating which object to grasp, when to return to the rest position, and when to stand up or sit. These instructions were accompanied by a static image of the current grasp type, which was intended as an undistracting reminder of the stimulus. When finishing a grasp series, an experimenter changed the object scene when necessary before resuming with the next grasp.

The *static* part of the exercise was followed by a *dynamic* one. This second part followed the same structure as the first, but in this case the grasp had to be used to perform a functional task with an object. The motivation for this variation was again to introduce variability into the data but this time by means of a dynamic, goal-oriented

Grasp		Object		Object Part		Vocal Instruction	Position
1	medium wrap	2	can	2	can	drink from the can	standing
		3	door handle	3	door handle	open and close the door handle	
2	lateral	5	key	5	key	turn the key in the lock	standing
		24	pencil case	6	zip	open and close the pencil case	
3	parallel extension	7	plate	7	plate	lift the plate	standing
		8	book	8	book	lift the book	
4	tripod grasp	1	bottle	10	cap	open and close the cap of the bottle	standing
		9	drawer	11	knob	open and close the drawer	
5	power sphere	12	ball	12	ball	move the ball to the right and back	standing
		5	key	5	key	move the keys forwards and backwards	
6	precision disk	15	jar	26	lid	open and close the lid of jar	seated
		13	bulb	13	bulb	screw and unscrew the light bulb	
7	prismatic pinch	16	clothespin	16	clothespin	squeeze the clothespin	seated
		5	key	27	keyring	move the keys forwards and backwards	
8	index finger extension	21	remote	17	button	press a button on the remote control	seated
		18	knife	18	knife	cut bread with the knife	
9	adducted thumb	20	screwdriver	20	screwdriver	turn the screwdriver	seated
		22	wrench	22	wrench	move the wrench to the right and back	
10	prismatic four finger	18	knife	18	knife	move the knife forwards and backwards	seated
		19	fork	19	fork	move the fork to the right and back	

Table 3. Overview of grasp types and objects for the *dynamic* condition of the exercise. The first four columns provide information as described in Table 2. The rightmost column indicates whether the movement was executed while seated or standing.

movement. As can be seen in Table 3, these functional movements reflect common activities with the combination of grasp type and object, such as drinking from a can held with a medium wrap. To limit the total duration of the exercise, the ten grasps were only combined with two objects each and executed either standing or seated. This position was chosen based on how the action would usually be performed in real life, for instance a door is more frequently opened while standing.

After the exercise finished the amputated subjects underwent three more exercises and a comprehensive questionnaire to investigate the neurocognitive effects of the amputation. The data and results of those exercises and the questionnaire will be published separately.

Post-Processing. Several processing steps were applied to the raw data acquired with the protocol described above. The objective of these steps was to sanitize the data, synchronize all modalities, and remove identifying information from the videos. In the following, we describe all procedures in detail.

Timestamp Correction. Due to an unfortunate implementation error, during a number of acquisitions the modalities were assigned timestamps from individual clocks. To unify all timestamps in a shared clock, the offset of all clocks was estimated and corrected with respect to the clock of the sEMG modality using statistics of their relative timing collected during trial acquisitions. Validations on the remaining unaffected acquisitions confirm that the maximum deviation of our estimate from the ground truth is less than 12 ms.

sEMG and Accelerometer Data. For computational efficiency, the sEMG and accelerometer streams from the Delsys Trigno device were acquired and timestamped in batches. During post-processing, individual timestamps were assigned to each sample via piecewise linear interpolation. A new piece is created if the linear model results in a deviation of more than 100 ms, which may happen if the fit is skewed due to missing or delayed data.

For the sEMG data, we furthermore filtered outliers by replacing samples that exceeded 30 standard deviations from the mean within a sliding window of 1 s with the preceding sample. The signals were subsequently filtered for power-line interference at 50 Hz (and its harmonics) using a Hampel filter, which interpolates the spectrum in processing windows only when it detects a clear peak³⁷. Contrary to the more common notch filter, this method does not affect the spectrum if there is no interference.

Gaze Data. The data from the Tobii Pro glasses were acquired as individually timestamped JavaScript Object Notation (JSON) messages. During post-processing, these messages were decoded and separated based on their type. Messages that arrived out-of-order were filtered and the resulting set of messages was used to determine the skew and offset between the computer clock and the one of the Tobii Pro glasses. This routine removes the constant part of the transmission delay as much as possible, while avoiding the possibility to antedate any events. The messages that relate directly to gaze information, such as gaze points, pupil diameter and so on, were then grouped together based on their timestamps.

Stimulus. The text-to-speech engine that was used to give vocal instructions introduced noticeable delays in the corresponding changes of the stimulus. We measured these delays for all sentences and languages, and moved the stimulus changes forward by these amounts during post-processing. Furthermore, small refinements were made to the *object* column, whereas its more specific *object-part* counterpart was calculated based on a fixed mapping from the original stimulus information.

Synchronization. For the standard data records (see the following section) all modalities were resampled at the original 1926 Hz sampling rate of the sEMG stream. For real-valued signals, this was done using a linear interpolation, while for discrete signals we used a nearest-neighbor interpolation. The signals that indicate the time and index of the MP4 video were handled separately using a custom routine, since they require to identify the exact change-point where one video transitions to the next.

Concatenation. The *static* and *dynamic* parts of the protocol were acquired independently and therefore produced separate sets of raw acquisition files. Furthermore, our acquisition protocol and software allowed to interrupt and resume the acquisition, either at request of the subject or to handle technical problems. After applying the previous processing steps to the individual acquisition segments, they were concatenated to obtain the standard data record. During this merging, we incremented the timestamps and video counter to ensure that they are monotonically increasing. Furthermore, if part of the protocol was repeated when resuming the acquisition, we took care to insert the novel segment at exactly the right place to avoid duplicate data.

Relabeling. The response of the subject and therefore the sEMG activation may not be aligned perfectly with the stimulus. As a consequence, the stimulus labels around the on- or offset of a grasp movement may be incorrect, resulting in an undue reduction in recognition performance. We addressed this shortcoming by realigning the stimulus boundaries with the procedure described by Kuzborskij *et al.*³⁸. In short, this method optimizes the log-likelihood of a rest-grasp-rest sequence on the whitened sEMG data within a feasible window that spans from 1 s before until 2 s after the original grasp stimulus. As opposed to the uniform prior used in the earlier method, we adopted a smoothed variant of the original stimulus label as prior. The advantage is that for trials without a clear difference in muscular activity during rest and the movement (i.e., the “evidence”), we recover the original label boundaries. Based on visual inspection of the updated movement boundaries, we assigned a certainty of $p = 0.6$ to this prior and selected a Gaussian filter with $\sigma = 0.5$ s as smoothing operator. The recalculated stimulus boundaries were saved in addition to the original ones.

Removing Identifying Information. All videos were checked manually for identifying information of anyone other than the experimenters. The segments of video that were marked as privacy-sensitive were subsequently anonymized with a Gaussian blur. In this procedure, we took care to re-encode only the private segments and to preserve the exact number and timestamps of all frames. In addition, the audio stream was removed from all videos for privacy reasons.

Data Records

The data that were acquired and processed with the described methodology are stored in the Harvard Dataverse repository³⁹. For each subject, this repository contains two data files in Matlab format (<http://www.mathworks.com>) and a series of corresponding videos encoded with MPEG-4 AVC in an MP4 container. The dataset³⁹ is provided with the *DatasetContentCRC.sfv* file, which contains a description of the dataset structure together with the Cyclic Redundancy Check (CRC) value for each file. This document can therefore be used to investigate how the dataset is structured as well as to verify the correctness of the downloaded data. The primary data file contains the concatenated sEMG data at their original sampling rate, to which all other modalities were resampled. An exhaustive listing of all the fields in these files together with a description is provided in Table 4. Further information regarding the content of the fields are described below:

- The fields *(re)grasp*, *(re)object*, and *(re)objectpart* contain the grasp, object, and objectpart IDs as described in Tables 2 and 3.
- The *emg* field typically (see the Usage Notes section) contains 12 columns: columns 1–8 refer to the signals of the electrodes forming the proximal array while columns 9–12 the signals of the electrodes forming the distal array.
- The same structure is maintained for the acceleration data in the *acc* field, in which groups of 3 columns are used to report the acceleration in the X, Y and Z axes for each electrode. In all the electrodes, the X axis is parallel to the forearm, the Z axis is orthogonal to the forearm surface, and the Y axis obeys the right-hand rule²⁸.
- The *gaze* field contains the position of the gaze point relative to the video frame expressed in (x, y) coordinates, having the origin of the coordinate system in the top left corner⁴⁰.
- The fields *gaze**point3D*, *pupilcenterleft*, *pupilcenterright*, *gazedirectionleft*, and *gazedirectionright* are expressed in (x, y, z) coordinates relative to the scene camera reference system, which has origin in the center of the camera, X axis pointing to the subject’s left, Y axis pointing upwards, and the Z axis obeying the right-hand rule⁴⁰. The *gazedirectionleft* and *gazedirectionright* fields are unit vectors, with the respective left and right pupil centers as origin.
- The angular velocity and the acceleration of the Tobii Glasses in the X, Y, and Z axes are contained in the *tobiigyr* and *tobiiaacc* fields⁴⁰.

Since resampling may not always be desirable due to its impact on the the signal spectrum, we also provide an auxiliary data file with all non-sEMG modalities at their original sampling rate. Each of these includes a

Field	Columns	Units	Description
grasp	1		ID of the desired grasp
grasprepetition	1		repetition counter for the desired grasp
object	1		ID of the target object
objectpart	1		ID of the target object part
objectrepetition	1		repetition counter for the target object
position	1		seated (0) or standing (1) position indicator
dynamic	1		static (0) or dynamic (1) grasp indicator
regrasp	1		realigned ID of the desired grasp
regrasprepetition	1		realigned repetition counter for the desired grasp
reobject	1		realigned ID of the target object
reobjectpart	1		realigned ID of the target object part
reobjectrepetition	1		realigned repetition counter for the target object
reposition	1		realigned subject position indicator
redynamic	1		realigned dynamic grasp indicator
acc	36	g	3-axis acceleration of the 12 electrodes
emg	12	V	myoelectric activity of the 12 electrodes
gazept	2		2D gaze point relative to the scene image
gazept_invalid	1		invalidity indicator for "gazept" (non-zero if invalid)
gazept3D	3	mm	3D gaze point in world coordinates
gazept3D_invalid	1		invalidity indicator for "gazept3D"
gazedirectionleft	3		3D gaze direction of the left eye
gazedirectionleft_invalid	1		invalidity indicator for "gazedirectionleft"
gazedirectionright	3		3D gaze direction of the right eye
gazedirectionright_invalid	1		invalidity indicator for "gazedirectionright"
pupilcenterleft	3	mm	3D position for the pupil center of the left eye
pupilcenterleft_invalid	1		invalidity indicator for "pupilcenterleft"
pupilcenterright	3	mm	3D position for the pupil center of the right eye
pupilcenterright_invalid	1		invalidity indicator for "pupilcenterright"
pupildiameterleft	1	mm	pupil diameter of the left eye
pupildiameterleft_invalid	1		invalidity indicator for "pupildiameterleft"
pupildiameterright	1	mm	pupil diameter of the right eye
pupildiameterright_invalid	1		invalidity indicator for "pupildiameterright"
tobiacc	3	m s ⁻²	3-axis acceleration of the Tobii
tobiacc_invalid	1		invalidity indicator for "tobiacc"
tobiigr	3	° s ⁻¹	3-axis angular velocity of the Tobii
tobiigr_invalid	1		invalidity indicator for "tobiigr"
tobiits	1	s	timestamp in the Tobii clock
vs	1	s	MP4 video timestamp
mp4videoidx	1		counter for the MP4 video
pts	1	s	TS presentation timestamp
tspipelineidx	1		TS pipeline ID
tsvideoidx	1		counter for the TS video
ts	1	s	timestamp in the computer clock

Table 4. Fields contained in the standard data record.

timestamp column, which can be used to synchronize them with each other or with the sEMG data in the primary data file. The fields and their detailed specification is shown in Table 5.

Technical Validation

Our intended purpose for the dataset is to investigate the fusion of sEMG with gaze behavior. In this section we therefore concentrate on validating these two modalities. Some of these analyses are low-level to ensure the quality of the recorded signals, while others are meant to verify that the data can in fact be used for the motivations and objectives for which they were created.

Gaze Data. Error Validation. The quality of gaze data primarily depends on the correctness of the initial calibration phase of the Tobii Pro glasses. Validating the effectiveness of this calibration consists of acquiring gaze data while the user is focused on a known target and subsequently comparing the measured gaze location with this ground truth^{41,42}. We used the data recorded during the calibration assessment described in the Acquisition Protocol section to evaluate the effectiveness of the calibration as well as possible quality degradation. These data

Field	Columns	Description
stimulus	1	timestamp in the computer clock
	2	ID of the desired grasp
	3	ID of the target object
	4	repetition counter for the desired grasp
	5	repetition counter for the target object
	6	seated or standing position
	7	ID of the target object part
	8	static or dynamic grasp
acc	1	timestamp in the computer clock
	2–37	3-axis acceleration of the 12 electrodes
gaze	1	timestamp in the computer clock
	2	timestamp in the Tobii clock
	3–4	2D gaze point relative to the scene image
	5	Tobii latency estimate
	6	invalidity indicator for 2D gaze point
	7–9	3D gaze point in world coordinates
	10	invalidity indicator for 3D gaze point
	11	pupil diameter of the left eye
	12	invalidity indicator for left pupil diameter
	13	pupil diameter of the left eye
	14	invalidity indicator for right pupil diameter
	15–17	pupil center of the left eye
	18	invalidity indicator for left pupil center
	19–21	pupil center of the right eye
22	invalidity indicator for right pupil center	
23–25	gaze direction of the left eye	
26	invalidity indicator for left gaze direction	
27–29	gaze direction of the right eye	
30	invalidity indicator for right gaze direction	
tobiacc	1	timestamp in the computer clock
	2	timestamp in the Tobii clock
	3	invalidity indicator for accelerometer data
	4–6	3-axis acceleration of the Tobii
tobiigr	1	timestamp in the computer clock
	2	timestamp in the Tobii clock
	3	invalidity indicator for gyroscope data
	4–6	3-axis angular velocity of the Tobii
vts	1	timestamp in the computer clock
	2	timestamp in the Tobii clock
	3	invalidity indicator for vts synchronization
	4	MP4 video timestamp
	5	counter for the MP4 video
pts	1	timestamp in the computer clock
	2	timestamp in the Tobii clock
	3	invalidity indicator for pts synchronization
	4	TS presentation timestamp
	5	TS pipeline ID

Table 5. Fields contained in each acquisition segment of the auxiliary data record with original sampling.

were typically collected at the beginning and end of an exercise. If the exercise was interrupted, the procedure was shown again before resuming it. We determined the ground truth by manually locating the cross position in pixels at intervals of 0.2 s using custom software. Since we also included calibration data for the other exercises done jointly as part the MeganePro project, a total of 498 acquisitions were processed in this manner.

The quality of eye tracking is often quantified in terms of accuracy and precision^{41,43}. For each axis, the former measures the systematic error, that is, the mean offset between the actual and expected gaze locations. Precision, on the other hand, measures the dispersion around the gaze position and thus the random error of the gaze point. In Fig. 2 these values are visualized with respect to the location within the video frame. This separation is intentional, as the eye tracking appears to be more accurate and precise in the center of the frame, namely

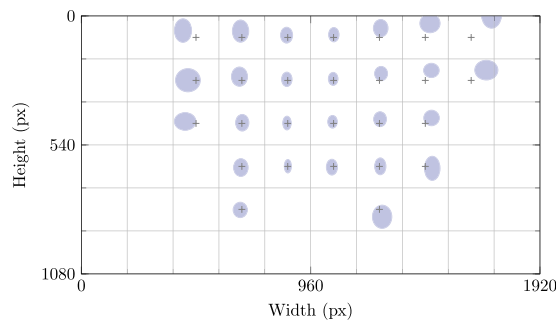


Fig. 2 The accuracy and precision of the eye tracking with respect to the location within the video frame. For each patch, the shift of the ellipse center with respect to the cross indicates the accuracy in either axis of the gaze within that patch. The radii of the ellipse on the other hand indicate the precision.

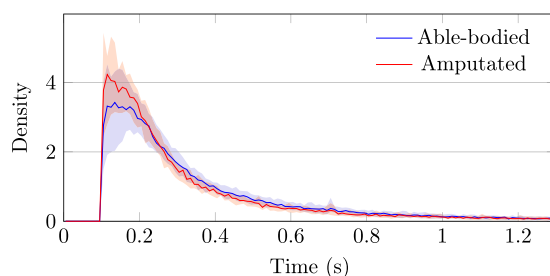


Fig. 3 Distribution of the fixation length histogram for able-bodied (blue) and amputated (red) subjects. The shaded areas indicate the 10th and 90th percentiles, while the solid line represents the median.

(-3.5 ± 19.4) px and (-1.5 ± 29.6) px on the x and y axes. Moving away from the center, the gaze results systematically shift towards the borders of the frame and its random error increases. We only visualize regions where we acquired at least 40 validation samples. Pooling all data, the overall accuracy and precision is (-0.8 ± 25.8) px and (-9.9 ± 33.6) px on the horizontal and vertical axes. At a typical manipulation distance of 0.8 m, this corresponds to a real-world precision and accuracy of approximately (-0.4 ± 11.5) mm and (-4.4 ± 14.9) mm. This is deemed sufficiently accurate considering the size of the household objects used in our experimental protocol.

To establish whether the calibration deteriorated over time, we compared the accuracy and precision collected at the beginning of an acquisition with those taken at the end. In total, we considered 210 uninterrupted acquisitions in which there was a calibration validation routine both at the beginning and the end. We found no statistically significant difference in accuracy (sign test, $p = 0.95$ and $p = 1.0$ in the horizontal and vertical axes) or precision (sign test, $p = 0.24$ and $p = 0.37$) indicating that drift does not pose an issue for the gaze data.

Statistical Parameters. To statistically describe a user's gaze behavior during the exercises and validate it against related literature, we first identified fixations and saccades in our eye tracking data using the Identification Velocity Threshold (IVT) method⁴⁴. To ensure that we could calculate the angular velocity of both eyes for a maximum number of samples, we linearly interpolated gaps of missing pupil data when shorter than 0.075 s⁴⁵. We used a threshold of 70°/s to discriminate between fixations and saccades⁴⁶. When the Tobii Pro glasses failed to produce a valid eye-gaze point, even after interpolating small gaps, the corresponding sample was marked as *invalid*. Excluding one subject who had strabismus, the percentage of such invalid samples ranged between (1.7 to 21.0)% and (4.3 to 30.7)% for able-bodied and amputated subjects. Sequences of events of the same type were then merged into segments identified by a time range and processed following the approach described by Komogortsev *et al.*⁴⁶. First, to filter noise or other disturbances, fixations separated by a short saccadic period of less than 0.075 s and 0.5° amplitude are merged. Second, fixations shorter than 0.1 s are marked as *invalid* and are excluded from the analysis.

In the resulting sequence of gaze events, the majority of invalid data are located between two periods of saccades, namely (92.2 ± 2.7)% and (92.6 ± 3.9)% for able-bodied and amputated subjects. This indicates that the Tobii Pro glasses fail predominantly to register high velocity data. Devices with sampling frequency lower than 250 Hz have indeed been categorized as “fixation pickers”⁴⁷ and often do not provide reliable results for all saccades. For this reason, in the following analysis we concentrate on fixation events.

Figure 3 shows the distribution of the duration of fixations for both types of subjects. The characteristics of these distributions, summarized in Table 6, coincide with those described in analogous studies^{21,48,49}. For instance, the mean values are similar to the mean duration of around 0.5 s reported by Hessels *et al.*⁵⁰. Moreover, both the median duration and the range between the 25th and 75th percentile are comparable with the results of Johansson *et al.*²¹, who report 0.286 s as median duration and (0.197 to 0.536) s as range between the same percentiles. These

Subjects	Mean [s]	Percentiles [s]		
		25 th	50 th	75 th
Able-bodied	0.429	0.170	0.260	0.470
Amputated	0.432	0.160	0.240	0.440

Table 6. Statistical parameters of the duration of fixations for able-bodied and amputated subjects.

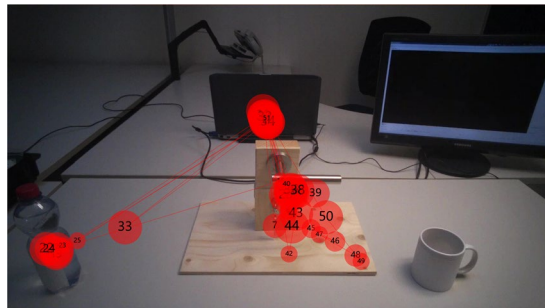


Fig. 4 Example of gaze points overlapped onto the scene camera video. Each circle represents a fixation, where the diameter indicates the duration of each fixation and the number the order of the fixations. In this case the subject was asked to grasp the door handle and the bottle.

similarities confirm the quality of the eye tracking data and highlight that the subjects maintained a natural gaze behavior throughout the exercise.

Since one of the intended uses of these data is to investigate gaze behavior in anticipation of object manipulation, we also verified that subjects indeed looked at the object when asked to manipulate it. With the help of an automated approach to detect objects, we determined for each grasp trial whether the distance between the gaze point and the boundary of the object of interest was at least once lower than 20 px. On average, this was the case in 95.9% of the subject's trials. Manual examination of the remaining 4.1% indicated that the fixation exceeded the distance 20 px not because of lack of subject engagement, but due to a low accuracy calibration of the Tobii Pro glasses. Regardless of this, in the vast majority of the trials the subjects visually located and fixated the object prior to its manipulation. For purely illustrative purposes, an example of gaze behavior of an able-bodied subject while grasping a door handle and a bottle is given in Fig. 4.

Myoelectric signals. Spectral Analysis. To assure the soundness of the recorded sEMG, we first analyzed the spectral properties and compared these with known results from the literature. For each subject and for each channel, we calculated the power spectral density via Welch's method with a Hann window of length 1024 (approximately 530 ms) and 50% overlap. Figure 5a shows the distribution over these densities via its median and the range between the 10th and 90th percentiles. The first observation is that nearly all of the energy of the signals is contained within (0 to 400) Hz, as is typical for sEMG⁵¹. Furthermore, there is no sign of powerline interference at 50 Hz or its harmonics, confirming the efficacy of the filtering approach detailed in the previous section.

We do however observe a rather large variability of densities among subjects and electrodes. The reason is that the spectrum and amplitude of sEMG depend on the exact position of an electrode over a muscle²⁴. In our protocol, none of the electrodes was positioned precisely on a muscle belly, thus causing a wide variety in the spectrum. In some cases, the signal may even be almost absent (e.g., an electrode over the radial bone).

The same variability is also noticeable in Fig. 5b, which reports the distribution of the median frequency over all subjects and electrodes throughout the entire exercise. The median frequencies we find are close to the approximately (120 to 130) Hz typically reported for the flexor digitorum superficialis^{52,53}, which is one of the muscles we primarily recorded from with our electrode positioning. Finally, we note that the distribution of the median frequency remains relatively stable over time, indicating that there are no persistent down- or upward shifts in the spectrum.

Grasp Classification. As a more high-level validation of the sEMG signals, we verify that these can indeed be used to discriminate the grasp a subject was performing, which is one of the anticipated applications of this dataset. We employ the standard window-based classification approach described by Englehart and Hudgins⁵⁴ with a window length of 400 samples (approximately 208 ms) and 95% overlap between successive windows. As feature-classifier combinations we consider:

- a (balanced) Linear Discriminant Analysis (LDA) classifier used with the popular four time-domain features⁵⁴;
- k-Nearest Neighbors (KNN) applied on RMS features⁵⁵; and
- Kernel Regularized Least Squares (KRLS) with a nonlinear exponential χ^2 kernel and marginal Discrete Wavelet Transform (mDWT) features^{55,56}.

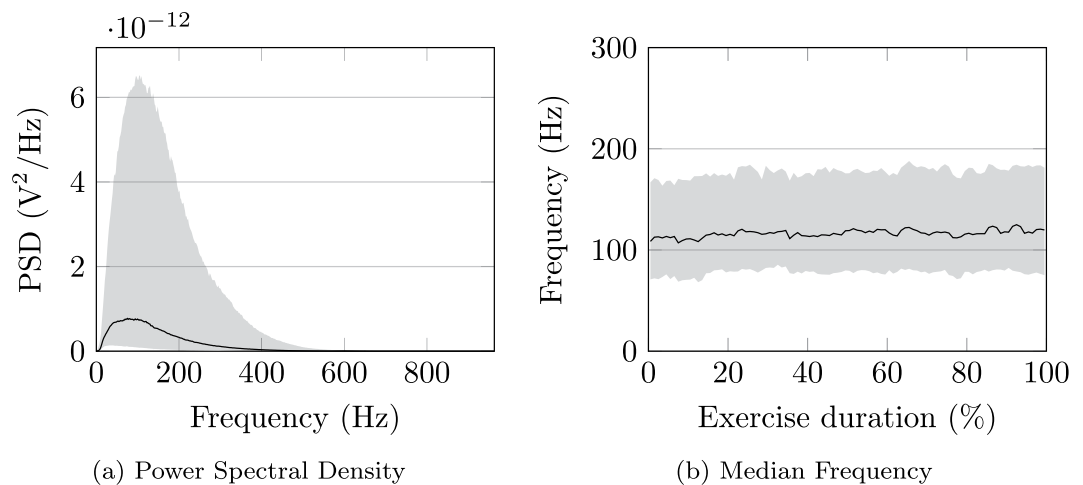


Fig. 5 The distribution of the power spectral densities and the median frequency throughout the duration of the exercise. The solid line indicates the median over all subjects and electrodes, while the shaded area indicates the 10th and 90th percentiles.

As commonly done in the field, a within-subject classification was performed. In contrast to prior work where we employed a single train-test split^{55,56}, the classification accuracy is defined here as the average accuracy of 4-fold cross validation. In each of these folds, one of the four repetitions per grasp-object-position combination was used as held-out test data, while the remaining three repetitions formed the training data. Similarly, any hyperparameters were optimized via nested 3-fold cross validation on the train repetitions. For all methods, the training data were downsampled with a factor of 10 for computational reasons, while the data used for hyperparameter optimization were downsampled with an additional factor of 4.

The results in Fig. 6 show a median classification accuracy between 63 and 82% for either able-bodied or amputated subjects, depending on the classification method. This is significantly higher than the approximately 50% accuracy a baseline classifier would achieve by simply predicting the most frequent *rest* class, confirming the discriminative power of the sEMG signals for the grasp type. Although a quantitative comparison with related work is of limited value due to discrepancies in experimental setup and protocol, the current results are a few percentage points higher than those presented by Atzori *et al.*⁵⁵. The most likely explanation is the lower number of grasps (i.e., only 10 rather than 40), which inevitably boosts performance. For amputees, the fact that we are considering subjects with different clinical parameters from previous studies may contribute to influence the performance difference, since it has been shown that remaining forearm length, phantom limb sensation intensity, and years passed since the amputation can influence the classification outcome⁵⁷.

Usage Notes

Relabeling. The data records come with both the original stimulus as well as a variant that has been aligned to actual sEMG activation (see the Post-Processing section). The latter variant is preferable when the stimulus is used as ground-truth of the grasp type, such as grasp recognition, since it reduces the number of incorrect labels due to response times. In other studies one may actually be interested in these response times, such as when investigating the psychophysical response to the vocal instruction. In these cases we advise users to use the original stimulus.

Trial Repetitions. In the experimental protocol, each new grasp started with two videos in first and third person perspective per object to introduce the subject to the grasp and the objects. Although subjects were encouraged to practice the grasps during this phase, some of them did not do this and focused on the video on the computer screen. For this reason, the hand and gaze behavior are unreliable and users of the dataset are advised to remove movements where the *(re)objectrepetition* column has a value of -3 or -2 .

sEMG & Accelerometer Data. A problem with sEMG and accelerometer data concerned electrode number 8 (the 8th column of the *emg* field and the 22nd, 23rd, and 24th columns of the *acc* field). Unfortunately, the data from this electrode seem unreliable. Myoelectric and accelerometer data recorded by this electrode sometimes have a substantially lower amplitude than the others, indicating a probable hardware issue. We therefore recommend to carefully consider this aspect when using the data.

Accelerometer data are known to be affected by systematic errors and noise. Therefore, we applied the method described in Tedaldi *et al.*⁵⁸ to estimate the calibration parameters for the accelerometers embedded in the Delsys Trigno electrodes as well as for the IMU of the Tobii glasses. The parameters and the original data are provided in the archive *accelerometer_calibration.tgz*.

S024. Due to the difficulties reported in the previous subsection, no myoelectric data were received from electrode number 8 during this acquisition. Therefore, the sEMG and accelerometer data for this subject were recorded from eleven electrodes instead of twelve.

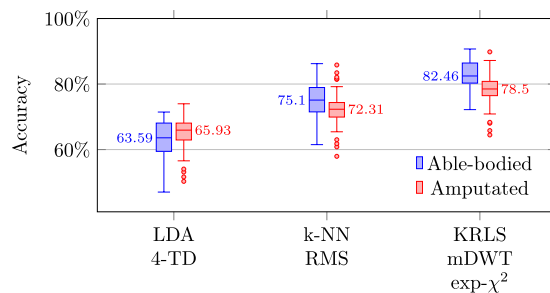


Fig. 6 Classification accuracies for able-bodied and amputated subjects when predicting the grasp type with three different types of classifiers.

S115 & S039. The small circumference of these participants' residual limb and forearm prevented the placement of 8 electrodes in the proximal array. For these two subjects only, the proximal array was composed of 7 electrodes and the distal one with the usual 4 electrodes. The corresponding *emg* field has therefore 11 columns instead of 12 as well as the *acc* field, which is composed of 33 columns and not 36 as for the other subjects.

S108. The high amputation level of S108 prevented the placement of the second array of electrodes. Therefore, only the first array consisting of eight electrodes was placed on the residual limb of this subject.

Gaze. It is known that various factors, such as physical characteristics of the test participant, recording environment, eye tracker features, and quality of calibration affect the gaze data quality⁴¹. The experiment was intentionally relatively unconstrained (e.g., the head was not fixed and subjects could move their torso) to encourage natural behavior. In the following cases we have identified potential problems with gaze data that may require consideration.

S111. A high percentage (~30%) of invalid gaze data were obtained for this subject. This is probably due to this participant's specific eye physiology, which is known to influence the tracking performance^{42,59}. The gaze data are included in the dataset for completeness.

S114. For this subject, calibration could not be performed due to strabismus. In such cases, the Tobii Pro glasses use a built-in default calibration. This allowed us to continue the experiment, but the quality of eye tracking is significantly worse⁴⁰. The difficulty in tracking the subject's eye in this particular condition is highlighted by the high proportion of invalid gaze samples (~50%). Although included in the dataset, the use of the gaze data for this subject should be carefully evaluated.

S115. A specific physical condition of this subject prevented a stable placement of the Tobii Pro glasses. The slippage compensation of the device may have helped to limit the consequences, as the proportion of invalid gaze samples (~10%) indicates a proper tracking of the eye. This condition should nonetheless be taken into account when analyzing the gaze and Tobii Pro glasses' IMU data for this subject.

Video. MPEG transport stream (MPEG-TS) videos were recorded wirelessly via the Tobii Pro glasses Application Programming Interface (API). The fields *pts*, *tspipelineidx*, and *tsvideoidx* of the data records serve to synchronize the data with these videos. We however release only the MP4 videos, this for two main reasons: to limit the size of the dataset and to ensure a high quality of the scene camera videos, since the MP4 videos were immune to packet loss problems.

Communication. Being able to select among four languages allowed the subjects to choose the one they were most comfortable with and, in most cases, it corresponded to their native language. For S111 only, none of the languages available in the acquisition software were appropriate. We were however able to communicate in Italian and, in case of difficulties, communication was facilitated by a relative of the subject translating from Italian to the subject's native language.

Code availability

The post-processing procedure described above was implemented in Matlab and executed in compiled form with Matlab 2016b. The relabeling procedure was implemented in Python and interpreted with Python 3.6. Censoring of the videos was done using a custom Bash script that interfaced with the FFmpeg 4.1.3 video manipulation tool. The GNU Parallel tool was used to run jobs in parallel⁶⁰. A copy of the code that was used to create the data records from the raw recordings is publicly available in the *megane_postprocess.tgz* archive within the MDSScript⁶¹. This archive also contains a *README* file that lists and describes the main processing steps. Although the original data files cannot be released for privacy reasons, the code is made available to allow the user to thoroughly investigate and comprehend the procedure we used to process the data as well as to provide the community with a tool that can be re-used and re-adapted for similar tasks.

Received: 9 August 2019; Accepted: 16 January 2020;
Published online: 10 February 2020

References

- Almécija, S., Smaers, J. B. & Jungers, W. L. The evolution of human and ape hand proportions. *Nat. Commun.* **6**, 7717 (2015).
- Kivell, T. L. Evidence in hand: Recent discoveries and the early evolution of human manual manipulation. *Philos. Trans. Royal Soc. B: Biol. Sci.* **370** (2015).
- Zecca, M., Micera, S., Carrozza, M. C. & Dario, P. Control of Multifunctional Prosthetic Hands by Processing the Electromyographic Signal. *Crit. Rev. Biomed. Eng.* **30**, 459–485 (2002).
- Castellini, C. *et al.* Proceedings of the first workshop on peripheral machine interfaces: Going beyond traditional surface electromyography. *Front. Neurobot.* **8**, 22 (2014).
- Hakonen, M., Piitulainen, H. & Visala, A. Current state of digital signal processing in myoelectric interfaces and related applications. *Biomed. Signal Process. Control.* **18**, 334–359 (2015).
- Resnik, L. *et al.* Evaluation of emg pattern recognition for upper limb prosthesis control: a case study in comparison with direct myoelectric control. *J. Neuroeng. Rehabil.* **15**, 23 (2018).
- Simon, A. M., Turner, K. L., Miller, L. A., Hargrove, L. J. & Kuiken, T. A. Pattern recognition and direct control home use of a multi-articulating hand prosthesis. In *IEEE International Conference on Rehabilitation Robotics (ICORR)*, 386–391 (IEEE, 2019).
- Scheme, E. & Englehart, K. Electromyogram pattern recognition for control of powered upper-limb prostheses: State of the art and challenges for clinical use. *J. Rehabil. Res. Dev.* **48**, 643–660 (2011).
- Jiang, N., Dosen, S., Muller, K. R. & Farina, D. Myoelectric Control of Artificial Limbs—Is There a Need to Change Focus? [In the Spotlight]. *IEEE Signal Process. Mag.* **29**, 152–150 (2012).
- Roche, A. D., Rehbaum, H., Farina, D. & Aszmann, O. C. Prosthetic Myoelectric Control Strategies: A Clinical. *Perspective. Curr. Surg. Reports* **2**, 44 (2014).
- Farina, D. *et al.* The extraction of neural information from the surface EMG for the control of upper-limb prostheses: emerging avenues and challenges. *IEEE Trans. Neural Syst. Rehabil.* **22**, 797–809 (2014).
- Vujaklija, I., Farina, D. & Aszmann, O. New developments in prosthetic arm systems. *Orthop. Res. Rev.* **8**, 31–39 (2016).
- Farina, D. & Amsüss, S. Reflections on the present and future of upper limb prostheses. *Expert. Rev. Med. Devices* **13**, 321–324 (2016).
- Cordella, F. *et al.* Literature review on needs of upper limb prosthesis users. *Front. Neurosci.* **10**, 209 (2016).
- Atzori, M. & Müller, H. Control capabilities of myoelectric robotic prostheses by hand amputees: a scientific research and market overview. *Front. Syst. Neurosci.* **9**, 162 (2015).
- Ghazaei, G., Alameer, A., Degenaar, P., Morgan, G. & Nazarpour, K. Deep learning-based artificial vision for grasp classification in myoelectric hands. *J. Neural Eng.* **14**, 036025 (2017).
- Castellini, C. & Sandini, G. Gaze tracking for robotic control in intelligent teleoperation and prosthetics. In *Proceedings of COGAIN - Communication via Gaze Interaction*, 73–77 (2006).
- Corbett, E. A., Kording, K. P. & Perreault, E. J. Real-time fusion of gaze and emg for a reaching neuroprosthesis. In *International Conference of the IEEE Engineering in Medicine and Biology Society (EMBC)*, 739–742 (IEEE, 2012).
- D'Avella, A. & Lacquaniti, F. Control of reaching movements by muscle synergy combinations. *Front. Comput. Neurosci.* **7** (2013).
- Giordaniello, F. *et al.* Megane Pro: myo-electricity, visual and gaze tracking data acquisitions to improve hand prosthetics. In *IEEE International Conference on Rehabilitation Robotics (ICORR)*, 1148–1153 (IEEE, 2017).
- Johansson, R. S., Westling, G., Bäckström, A. & Flanagan, J. R. Eye–hand coordination in object manipulation. *J. Neurosci.* **21**, 6917–6932 (2001).
- Land, M. F. Eye movements and the control of actions in everyday life. *Prog. Retin. Eye Res.* **25**, 296–324 (2006).
- Desanghere, L. & Marotta, J. J. The influence of object shape and center of mass on grasp and gaze. *Front. Psychol.* **6**, 1537 (2015).
- De Luca, C. J. The use of surface electromyography in biomechanics. *J. Appl. Biomech.* **13**, 135–163 (1997).
- Merletti, R., Rainoldi, A. & Farina, D. Myoelectric manifestations of muscle fatigue. In *Electromyography: Physiology, Engineering, and Noninvasive Applications*, (eds Merletti, R. & Parker, P.) Ch. 9 (John Wiley & Sons Ltd., 2005).
- Kyranou, I., Vijayakumar, S. & Erden, M. S. Causes of performance degradation in non-invasive electromyographic pattern recognition in upper limb prostheses. *Front. Neurobot.* **12**, 58 (2018).
- Atzori, M. *et al.* Electromyography data for non-invasive naturally-controlled robotic hand prostheses. *Sci. Data* **1**, 140053 (2014).
- Delsys Inc. Trigno Wireless System User's Guide (2016).
- Cognolato, M., Atzori, M. & Müller, H. Head-mounted eye gaze tracking devices: an overview of modern devices and recent advances. *J. Rehabil. Assist. Technol. Eng.* **5** (2018).
- Pizzolato, C. *et al.* CEINMS: A toolbox to investigate the influence of different neural control solutions on the prediction of muscle excitation and joint moments during dynamic motor tasks. *J. Biomech.* **48**, 3929–3936 (2015).
- Cutkosky, M. R. On grasp choice, grasp models, and the design of hands for manufacturing tasks. *IEEE Trans. Robot. Autom.* **5**, 269–279 (1989).
- Sebelius, F. C. P., Rosen, B. N. & Lundborg, G. N. Refined myoelectric control in below-elbow amputees using artificial neural networks and a data glove. *J. Hand Surg.* **30**, 780–789 (2005).
- Crawford, B., Miller, K. J., Shenoy, P. & Rao, R. P. N. Real-time classification of electromyographic signals for robotic control. In *Proceedings of the Twentieth National Conference on Artificial Intelligence and the Seventeenth Innovative Applications of Artificial Intelligence Conference*, 523–528 (AAAI Press, 2005).
- Feix, T., Romero, J., Schmiedmayer, H. B., Dollar, A. M. & Kragic, D. The GRASP taxonomy of human grasp types. *IEEE Trans. Hum.-Mach. Syst.* **46**, 66–77 (2016).
- Bullock, I. M., Zheng, J. Z., De La Rosa, S., Guertler, C. & Dollar, A. M. Grasp frequency and usage in daily household and machine shop tasks. *IEEE Trans. Haptics* **6**, 296–308 (2013).
- Hargrove, L. J., Englehart, K. & Hudgins, B. A comparison of surface and intramuscular myoelectric signal classification. *IEEE Trans. Biomed. Eng.* **54**, 847–853 (2007).
- Allen, D. P. A frequency domain hamper filter for blind rejection of sinusoidal interference from electromyograms. *J. Neurosci. Methods* **177**, 303–310 (2009).
- Kuzborskij, I., Gijsberts, A. & Caputo, B. On the challenge of classifying 52 hand movements from surface electromyography. In *International Conference of the IEEE Engineering in Medicine and Biology Society (EMBC)*, 4931–4937 (IEEE, 2012).
- Cognolato, M. *et al.* MeganePro dataset 1 (MDS1). *Harvard Dataverse*. <https://doi.org/10.7910/DVN/1Z3IOM> (2019).
- Tobii AB. Tobii Pro Glasses 2 API Developer's Guide. (2016).
- Holmqvist, K., Nyström, M. & Mulvey, F. Eye tracker data quality: What it is and how to measure it. In *Proceedings of the Symposium on Eye Tracking Research and Applications (ETRA)*, (ACM, 2012).
- Blignaut, P. & Wium, D. Eye-tracking data quality as affected by ethnicity and experimental design. *Behav. Res. Methods* **46**, 67–80 (2014).
- Reingold, E. M. Eye tracking research and technology: towards objective measurement of data quality. *Vis. Cogn.* **22**, 635–652 (2014).
- Salvucci, D. D. & Goldberg, J. H. Identifying fixations and saccades in eye-tracking protocols. In *Proceedings of the Symposium on Eye Tracking Research and Applications (ETRA)*, (ACM, 2000).
- Olsen, A. The tobii i-vt fixation filter. Technical report, Tobii Technology (2012).

46. Komogortsev, O. V., Gobert, D. V., Jayarathna, S., Koh, D. H. & Gowda, S. M. Standardization of automated analyses of oculomotor fixation and saccadic behaviors. *IEEE Trans. Biomed. Eng.* **57**, 2635–2645 (2010).
47. Karn, K. S. “saccade pickers” vs. “fixation pickers”: the effect of eye tracking instrumentation on research. In *Proceedings of the Symposium on Eye Tracking Research and Applications (ETRA)*, (ACM, 2000).
48. Kinsman, T., Evans, K., Sweeney, G., Keane, T. & Pelz, J. Ego-motion compensation improves fixation detection in wearable eye tracking. In *Proceedings of the Symposium on Eye Tracking Research and Applications (ETRA)*, (ACM, 2012).
49. Duchowski, A. T. *Eye Tracking Methodology: Theory and Practice*. (Springer-Verlag, 2003).
50. Hessels, R. S., Niehorster, D. C., Kemner, C. & Hooge, I. T. Noise-robust fixation detection in eye movement data: Identification by two-means clustering (i2mc). *Behav. Res. Methods* **49**, 1802–1823 (2017).
51. Basmajian, J. V. & De Luca, C. J. *Muscles Alive*. 5th edn (Williams & Wilkins, 1985).
52. Clancy, E. A., Bertolina, M. V., Merletti, R. & Farina, D. Time- and frequency-domain monitoring of the myoelectric signal during a long-duration, cyclic, force-varying, fatiguing hand-grip task. *J. Electromyogr. Kinesiol* **18**, 789–797 (2008).
53. Kattla, S. & Lowery, M. M. Fatigue related changes in electromyographic coherence between synergistic hand muscles. *Exp. Brain Res.* **202**, 89–99 (2010).
54. Englehart, K. & Hudgins, B. A robust, real-time control scheme for multifunction myoelectric control. *IEEE Trans. Biomed. Eng.* **50**, 848–854 (2003).
55. Atzori, M., Gijsberts, A., Müller, H. & Caputo, B. Classification of hand movements in amputated subjects by semg and accelerometers. In *International Conference of the IEEE Engineering in Medicine and Biology Society (EMBC)*, 3545–3549 (IEEE, 2014).
56. Gijsberts, A., Atzori, M., Castellini, C., Müller, H. & Caputo, B. Movement error rate for evaluation of machine learning methods for semg-based hand movement classification. *IEEE Trans. Neural Syst. Rehabil* **22**, 735–744 (2014).
57. Atzori, M. *et al.* Clinical parameter effect on the capability to control myoelectric robotic prosthetic hands. *J. Rehabil. Res. Dev.* **53**, 345–358 (2016).
58. Tedaldi, D., Pretto, A. & Menegatti, E. A robust and easy to implement method for IMU calibration without external equipments. In *Proceedings of the IEEE International Conference on Robotics and Automation (ICRA)*, 3042–3049 (IEEE, 2014).
59. Nyström, M., Andersson, R., Holmqvist, K. & van de Weijer, J. The influence of calibration method and eye physiology on eyetracking data quality. *Behav. Res. Methods* **45**, 272–288 (2013).
60. Tange, O. Gnu parallel - the command-line power tool.;login: *The USENIX Magazine* **36**, 42–47 (2011).
61. Gijsberts, A. & Cognolato, M. MeganePro Script Dataset (MDSScript). *Harvard Dataverse*. <https://doi.org/10.7910/DVN/2AEB6C> (2019).

Acknowledgements

This work was supported by the Swiss National Science Foundation Sinergia project #160837 “MeganePro” and by the Hasler Foundation in the project ELGAR PRO. We thank the subjects for their participation in the Myo-Electricity, Gaze And Artificial-intelligence for Neurocognitive Examination & Prosthetics (MeganePro) project. We thank Prof. G. Pajardi, Dr. E. Rosanda, and the team of the hand surgery and rehabilitation department of the Ospedale San Giuseppe MultiMedica Group in Milan, Italy for their help in recruiting subjects for this study. Furthermore, we thank Mara Graziani, Francesca Giordaniello, and Francesca Palermo for their help in developing a preliminary version of the acquisition protocol and testing the acquisition software.

Author contributions

M.C. created the acquisition protocol, developed the acquisition software, performed data acquisition, and wrote the paper. A.G. created the acquisition protocol, developed the post-processing procedure and software, performed data analysis, and wrote the paper. V.G. created the acquisition protocol, performed data analysis, and wrote the paper. G.S. helped with the creation of the acquisition protocol and with the data acquisition, obtained ethical approval, and reviewed the paper. K.G. recruited the participants, helped with the data acquisition, checked the videos for private data, and reviewed the paper. A.-G.M.H., C.T. and F.B. recruited the participants and reviewed the paper. A.G. helped with the post-processing software, performed data analysis, and reviewed the paper. D.F. recruited the participants, helped with the data acquisition and reviewed the paper. B.C., P.B. and H.M. ideated the project and reviewed the paper. M.A. ideated the project, created the acquisition protocol, obtained ethical approval, helped with the data acquisition, and reviewed the paper.

Competing interests

The authors declare no competing interests.

Additional information

Correspondence and requests for materials should be addressed to M.C., M.A. or H.M.

Reprints and permissions information is available at www.nature.com/reprints.

Publisher’s note Springer Nature remains neutral with regard to jurisdictional claims in published maps and institutional affiliations.



Open Access This article is licensed under a Creative Commons Attribution 4.0 International License, which permits use, sharing, adaptation, distribution and reproduction in any medium or format, as long as you give appropriate credit to the original author(s) and the source, provide a link to the Creative Commons license, and indicate if changes were made. The images or other third party material in this article are included in the article’s Creative Commons license, unless indicated otherwise in a credit line to the material. If material is not included in the article’s Creative Commons license and your intended use is not permitted by statutory regulation or exceeds the permitted use, you will need to obtain permission directly from the copyright holder. To view a copy of this license, visit <http://creativecommons.org/licenses/by/4.0/>.

The Creative Commons Public Domain Dedication waiver <http://creativecommons.org/publicdomain/zero/1.0/> applies to the metadata files associated with this article.

© The Author(s) 2020